Acervo ISA

INSTITUTO SOCIOAMBIENTAL
data ____/____/____
cod. 16D 00002 2

INT. J. REMOTE SENSING, 1997, VOL. 18, NO. 3, 663–670

Identification and mapping of the Amazon habitats using a mixing model

E. M. NOVO and Y. E. SHIMABUKURO

Instituto Nacional de Pesquisas Espaciais—INPE, Av. dos Astronautas, 1758, São José dos Campos, São Paulo, 12227-010, Brazil

(*Received 3 July 1995; in final form 24 July 1996*)

Abstract. A methodology is described for identifying and mapping floodplain habitats in a reach of the Amazon mainstream. A linear mixing approach was used to determine the fraction of three pure endmembers. This method was tested for two radiometrically rectified Landsat Thematic Mapper (TM) scenes and the proportions of endmembers were used to identify the following classes: (1) clear/mixed water; (2) turbid water; (3) flooded non-forest; (4) flooded forest; (5) human settlements and (6) aquatic vegetation. The results were compared to visually interpreted Landsat TM images.

1. Introduction

There is increasing concern that the buildup of greenhouse gases (GHG) in the atmosphere is leading to global warming. Among them, the concentrations of CO_2 and CH_4 are expected to increase in the future because they are related to food and energy conversion. Methane is considered a high priority GHG because its concentration is increasing at a rate of about 1 per cent a year over the last 15 years (OECD 1993).

The Amazon floodplain wetlands are well known as natural sources of methane to the atmosphere (Bartlett *et al.* 1988, 1990, Devol *et al.* 1988). The magnitude of its emissions is doubtful, however, due to the lack of information on the temporal and spatial variability of sources (Bartlett *et al.* 1990). Measurements performed in the Brazilian Amazon since 1985 show significant differences in the methane flux in the floodplain habitats: open water, grass mats and flooded forest (Bartlett *et al.* 1990). The area covered by those habitats, however, is poorly known and varies seasonally.

Quantitative estimates of the area covered by floodplain habitats based on Landsat TM data are limited to restricted areas (Mertes *et al.* 1995). One of the major problems of using TM for mapping the entire Amazon floodplain is related to the signature extension from one scene to another from different acquisition dates and paths. Changes in atmospheric and environmental conditions (water level, water colour, vegetation phenology, etc.) even for contiguous areas make it difficult to map the entire Amazon floodplain, specially for digital data analysis.

This letter describes a methodology for mapping the floodplain habitats using Landsat TM images based on the application of a mixing model (Shimabukuro and Smith 1991) to determine the fraction of three pure endmembers accounting for the digital numbers of the pixels found in the floodplain environment.

0143–1161/97 $12.00 © 1997 Taylor & Francis Ltd

Acervo ISA

2. Methodology

2.1. *Study area*

The study area covers the reach of the Amazon floodplain extending from Manaus to Itacoatiara (figure 1). This floodplain reach consists of a mixture of different vegetation types ranging from floodplain forest to grassland (Departamento Nacional de Produção Mineral 1976). In this region, two main transitions can be observed: in the west region, the transition is between the herbaceous and savanna like

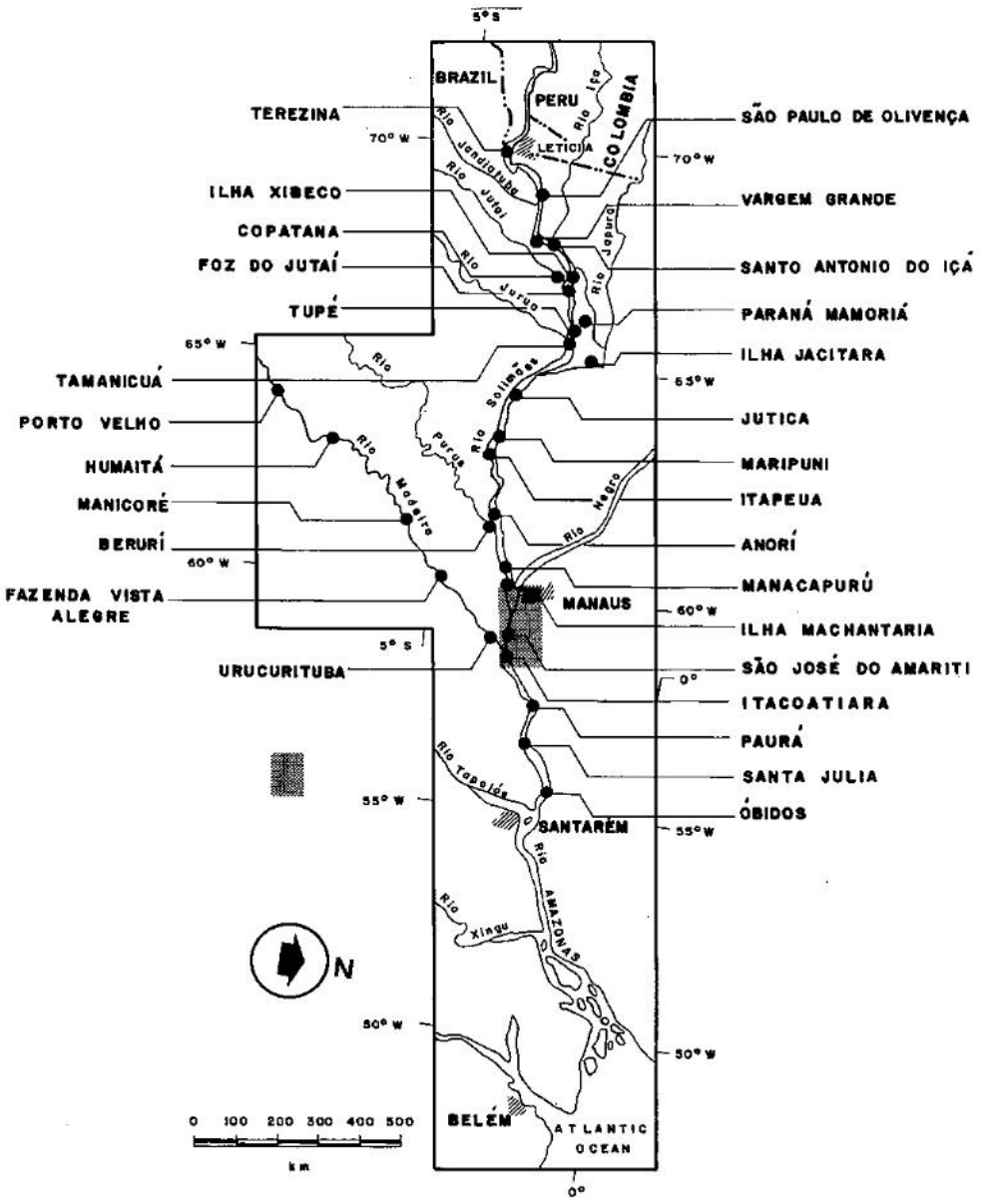

Figure 1. Test site location.

vegetation and the floodplain forest; and in the east region, the transition is between herbaceous vegetation and grassland.

2.2. *Data set*

Two adjacent Landsat TM (path 229/row 062 and path 230/row 062) scenes were used in this study. They were available in the digital format (bands 1 to 5) and correspond to the high water period, i.e. 229/062 was acquired on 10 August 1991 and 230/062 was acquired on 2 July 1992.

2.3. *Procedures*

The study was conducted as follows: (1) transformation of the image digital numbers into reflectance; (2) application of radiometric rectification; (3) assessment of the rectification process; (4) application of the mixing model; and (5) classification of the floodplain habitats.

2.3.1. *Transformation of the image digital numbers into reflectance*

The transformation of the image digital numbers into reflectance values was performed according to Markham and Barker (1986) as follows:

$$L_\lambda = L_{\min\lambda} + \left(\frac{L_{\max\lambda} - L_{\min\lambda}}{\mathrm{QCAL}_{\max\lambda}}\right)\mathrm{QCAL} \tag{1}$$

where: L_λ is spectral radiance, $L_{\min\lambda}$ is minimum spectral radiance, $L_{\max\lambda}$ is maximum spectral radiance, $\mathrm{QCAL}_{\max}$ is digital number range, and QCAL is digital number and

$$\rho_p = \frac{\pi L_\lambda d^2}{E_{\mathrm{sun}\,\lambda}\cos\theta s} \tag{2}$$

where: ρ_p is apparent reflectance, L_λ is spectral radiance ($\mathrm{mW\,cm^{-2}\,sr^{-1}\,\mu m^{-1}}$), d is Sun–Earth distance in astronomical units, $E_{\mathrm{sun}\,\lambda}$ is exoatmospheric average spectral radiance ($\mathrm{mW\,cm^{-2}\,\mu m^{-1}}$), and θ_s is Sun zenith angle.

2.3.2. *Application of a radiometric rectification to the images*

The radiometric rectification algorithm is based on the method developed by Hall *et al.* (1991) as follows: (1) acquisition of radiometric control sets with little or no variation in the mean surface reflectance between images; and (2) empirical determination of coefficients for linear transformation of all images in relation to a reference data set. The model used in the rectification is given by a set of linear transforms as follows:

$$T = m_i + b_i \tag{3}$$

where:

$$m_i = (Br_i - Dr_i)/(Bs_i - Ds_i)$$

$$b_i = (Dr_i Bs_i - Ds_i Br_i)/(Bs_i - Ds_i)$$

and Br_i is the average of the bright reference set, Dr_i is the average of the dark reference set, Bs_i is the average of the bright subject set, and Ds_i is the average of the dark subject set.

The rectification transform coefficients (m_i and b_i) are shown in table 1.

Acervo ISA

Table 1. Rectification transform coefficients between 229/062 and 230/062 images.

	Band 1	Band 2	Band 3	Band 4	Band 5
m_i	3·473	−2·537	3·614	1·077	3·614
b_i	−60·529	67·224	−40·625	−7·528	−1·617

2.3.3. *Assessment of the rectification process*

To assess the rectification process a series of samples were randomly collected in the reference image (*Ref*), original image to be rectified (*Ori*) and in the rectified image (*Rec*) and a t test was applied to the data as follows:

(a) H_0 = There is no significant difference between the digital numbers of the original image and the rectified image in bands TM1, TM2, TM3, TM4 and TM5.
H_1 = There is significant difference between the digital numbers of the original image and the rectified image in bands TM1, TM2, TM3, TM4 and TM5.

The t values for testing this hypothesis are presented in table 2. The critical t for a $\alpha = 0{\cdot}001$ and 98 degrees of freedom is 2·66, indicating that there are significant differences in the average DN of the *Ori* and *Rec* images, showing that the rectification do affect the reflectance distribution of the output. The samples were collected in regions of the image classified as forest because it was assumed that it would be less subjected to inherent changes from one date to another.

(b) H_0 = There is no significant difference between the rectified image (*Rec*) and the reference image (*Ref*).
H_1 = There is significant difference between the rectified image and the reference image.

The t values for testing this hypothesis were computed for the five TM bands using the average of three random 100 pixel sample areas taken in forested areas (table 3). The critical t for a $\alpha = 0{\cdot}001$ and 4 degrees of freedom is 4·60. Data on table 3 indicate that there are no significant differences in the average DN of the *Ref* and *Rec* images, showing that it is possible to use the same set of endmembers to classify the floodplain habitats.

2.3.4. *Application of the mixing model to the rectified images*

The selected endmembers for this study were: vegetation, water/shade and soil. After the radiometric rectification the same set of endmembers were applied to both reference and rectified images. The digital numbers describing each endmember are

Table 2. Computed t values for random samples collected in the original and rectified images.

	t value TM1	t value TM2	t value TM3	t value TM4	t value TM5
Sample 1	48·4154	−33·6403	39·8519	8·05201	3·04629
Sample 2	47·0810	−35·2427	34·6706	7·43273	3·21688
Sample 3	38·0890	−15·2823	27·5843	5·88659	3·19759
Sample 4	25·4823	−15·5196	29·8165	5·41823	2·24725
Sample 5	14·8175	11·3907	12·4589	6·08068	2·49760

Table 3. Computed t values for random samples collected in the reference and rectified images.

TM band	t value
TM1	2·43926
TM2	0·31947
TM3	3·81554
TM4	0·61230
TM5	0·550921

Table 4. Digital numbers equivalent to the spectral reflectance of the pure endmembers.

	TM1	TM2	TM3	TM4	TM5
Veg.	20	21	14	103	38
Soil	42	60	80	93	118
Water	17	12	9	5	0

shown in table 4. The vegetation endmember represents the signature of green dense vegetation, the soil endmember represents areas with low vegetation cover where the soil is the main item responsible for the pixel reflected radiance. Shade/water endmember represents the darkest pixel found in the image with a spectral behaviour similar to shade or pure water (digital numbers decreasing from shorter to larger wavelengths).

Theoretically, the digital number of each floodplain habitat can be described by the proportion of these three pure endmembers, i.e. tropical forest would have a high proportion of vegetation, a medium proportion of shade and a null proportion of soil, whereas a black water would have a low proportion of both vegetation and soil and a high proportion of shade/water endmember.

The mixing model can be expressed as follows:

$$r_i = a \times \text{veg}_i + b \times \text{soil}_i + c \times \text{water}_i + e_i \quad (4)$$

where: r_i is reflectance of a given pixel in the ith band, a is proportion of vegetation in a given pixel, veg_i is reflectance of the vegetation in the ith band, b is proportion of soil in a given pixel, soil_i is reflectance of the soil in the ith band, c is proportion of water or shade in a given pixel, water_i is reflectance of the water in the ith band, and e_i is error in the ith band.

2.3.5. *Classification of floodplain habitats*

A map derived from visually interpreted TM images was used as a reference (Novo *et al.* 1996) for classification of floodplain habitats. Several samples of different habitats were collected with the aid of that reference map and used to determine the fractions of endmember for characterizing each class. Table 5 presents the class intervals used in the floodplain habitat classification.

3. Results

Figure 2 shows the spatial distribution of the floodplain habitats derived from the mixing model and figure 3 presents that derived from visual interpretation. There are striking differences among them: (1) the area occupied by the class flooded forest is underestimated in the visual interpretation map because most of the narrow

Acervo ISA

Table 5. Digital number class intervals equivalent to the fraction of pure endmembers of each floodplain habitat.

	Vegetation fraction	Soil fraction	Water fraction
Clear/mixed water	⩾90 and ⩽115	⩾90 and ⩽115	⩾195 and ⩽200
Turbid water	⩾90 and ⩽115	⩾90 and ⩽115	⩾185 and ⩽194
Flooded non-forest	⩾120 and ⩽185	⩾120 and ⩽185	⩾105 and ⩽155
Flooded forest	⩾130 and ⩽180	⩾80 and ⩽100	⩾125 and ⩽160
Human settlements	⩾80 and ⩽170	⩾130 and ⩽200	⩾80 and ⩽140
Aquatic vegetation	⩾90 and ⩽180	⩾70 and ⩽125	⩾161 and ⩽195

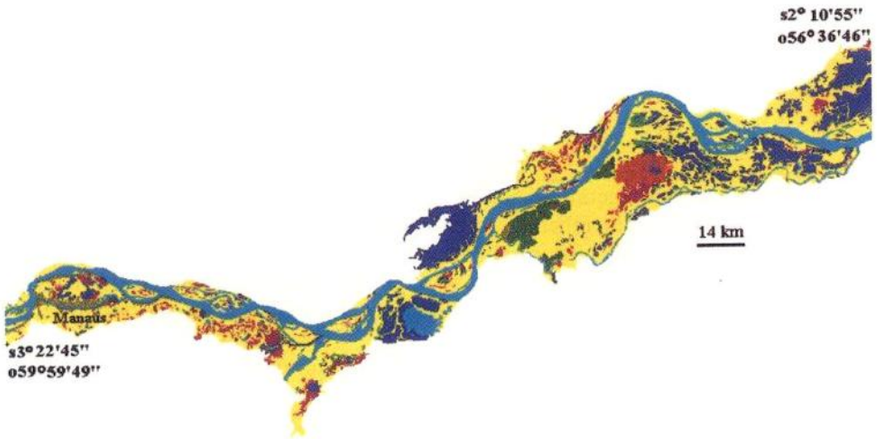

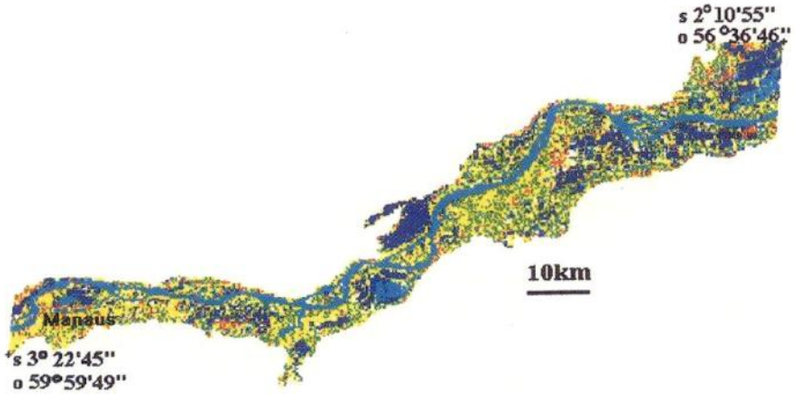

Figure 2. (top) Floodplain habitats based on the classification of the fractions of three endmembers: vegetation, soil and shade/water. Clear/mixed water (blue), turbid water (cyan), flooded non-forest (yellow), flooded forest (green), human settlements (red), and aquatic vegetation (white).

Figure 3. (bottom) Floodplain habitats derived from visual interpretation of TM/Landsat data. Clear/black water (magenta), mixed water (blue), turbid water (cyan), flooded non-forest (yellow), flooded forest (green), aquatic vegetation (dark green) and not classified (black).

stretches of forest in the river banks were not mapped; (2) three water types were mapped in the visual interpretation (black/clear, turbid and intermediate) based on tonal changes, but only two types of water could be mapped (black/clear, turbid water) using the mixing model approach.

Those differences can be explained by the following factors: (1) the images used in the visual interpretation were not submitted to radiometric rectification, being standard colour prints enhanced to provide the best contrast for detection of deforested areas; (2) the image scale (1:250 000) was not adequate to map the small scale patterns found in the floodplain.

New approaches, such as intense field trips in selected test sites, for assessing the accuracy of this methodology are being pursued (Mertes *et al.* 1995, 1996) in order to extend this methodology to the entire Amazon basin.

4. Conclusions

The proposed methodology can be used to digitally classify the floodplain habitats using several Landsat TM scenes. The radiometric rectification procedure minimized the difference of spectral responses between the two adjacent TM scenes allowing for the application of the mixture algorithm using only one set of endmembers. The accuracy of this method was not determined but a methodology to do so is being pursued.

Acknowledgments

The authors acknowledge the National Institute for Space Research for supporting this study and Dr João Vianei Soares for comments and suggestions.

References

Bartlett, K. B., Crill, P. M., Sebacher, D. I., Harriss, R. C., Wilson, J. O., and Melack, J. M., 1988, Methane flux from the central Amazonian floodplain. *Journal of Geophysical Research*, **93,** 1571–1582.

Bartlett, K. B., Crill, P. M., Bonassi, J. A., Richey, J. E., and Harris, R. C., 1990, Methane flux from the Amazon river floodplain: emissions during rising water. *Journal of Geophysical Research*, **95,** 16 773–16 788.

Departamento Nacional de Produção Mineral. Projeto RADAMBRASIL, 1976, Folha SA.21-Santarém, Rio de Janeiro, Brasil, p. 510.

Devol, A. H., Richey, J. E., Clarck, W. A., King, S. L., and Martinelli, L. A., 1988, Methane emissions to the troposphere. *Journal of Geophysical Research*, **93,** 1583–1592.

Hall, F. G., Strebel, D. E., Nickeson, J. E., and Goetz, S. J., 1991, Radiometric rectification: toward a common radiometric response among multidate, multisensor images. *Remote Sensing of Environment*, **35,** 11–27.

Markham, B. L., and Barker, J. L., 1986, Landsat MSS and TM post-calibration dynamic ranges exoatmospheric reflectances and at-satellite temperatures. Landsat User Notes, EOSAT. Lanham, MD.

Mertes, L. A. K., Daniel, D. L., Melack, J. M., Nelson, B., Martinelli, L. A., and Forsberg, B. R., 1995, Spatial patterns of hydrology, geomorphology, and vegetation on the floodplain of the Amazon River in Brazil from a remote sensing perspective. *Geomorphology*, **13,** 15–232.

Mertes, L. A. K., Novo, E. M. L. M., Daniel, D. L., Shimabukuro, Y. E., Richey, J. E., and Krug, T., 1996, Classification of Rio Solimões—Amazonas wetlands through the application of spectral mixture analysis to Landsat Thematic Mapper data. *VIII Simpósio Brasileiro de Sensoriamento Remoto, INPE, São José dos Campos*, pp. 61–65.

Novo, E. M. L. M., Leite, F. A., Ávila, J., Ballester, V., and Melack, J., 1996, Assessment of Amazon floodplain habitats using TM/Landsat data. *Revista Ciência e Cultura* (in press).

Acervo ISA

ORGANIZATION FOR ECONOMIC COOPERATION AND DEVELOPMENT (OECD), 1993, National GHG Inventories: Transparency in estimation and reporting. Intergovernmental panel on climate change, WMO, YNEP.

SHIMABUKURO, Y. E., and SMITH, J. A., 1991, The least-squares mixing models to generate fraction images derived from remote sensing multispectral data. *I.E.E.E. Transactions on Geoscience and Remote Sensing*, **29**, 16–20.